Proceedings of ASME Turbo Expo 2011
GT2011
June 6-10, 2011, Vancouver, British Columbia, Canada

GT2011-45086

NOVEL APPROACH FOR LOSS AND FLOW-TURNING PREDICTION USING OPTIMIZED SURROGATE MODELS IN TWO-DIMENSIONAL COMPRESSOR DESIGN

Andreas Schmitz, Marcel Aulich and Eberhard Nicke
German Aerospace Center
Institute of Propulsion Technology
Fan and Compressor Department
51147 Cologne, Germany
andreas.schmitz@dlr.de marcel.aulich@dlr.de eberhard.nicke@dlr.de

ABSTRACT

Two-dimensional (2D) streamline curvature methods are still an important tool in modern compressor design. In the past most of the streamline curvature methods made use of empirical correlations to approximate the blade row losses and deviation functions on which the accuracy of streamline curvature methods mainly depend. These empirical correlations are just accurate for a small set of geometric airfoil design parameters for which they where obtained and the prediction of airfoil performance at high Mach numbers or at off-design condition is inaccurate. Nowadays, a new approach is needed to consider highly customized, modern airfoil geometries with an increased number of design parameters. A new method with the possibility to predict the performance of these highly customized airfoils also at off-design condition and high Mach numbers is presented in this paper. This method uses a large airfoil database together with optimized surrogate models to accurately predict airfoil performance. The database consists of approximately 10^6 randomly created airfoils with randomly created inflow conditions and the airfoil performance which results from the 2D Euler-boundary layer code MISES [16]. The airfoil geometry in this database is described by ten geometrical parameters, e.g. stagger angle, chord length etc.. The flow condition is described by four flow parameters such as the relative inflow Mach number, MVDR, relative inflow angle and Reynolds number. Airfoil performance is represented by total pressure loss and flow-turning. This database was used to train neural networks that provides the relationship between the geometrical/flow parameters and the airfoil performance. The topology of the neural networks was optimized to achieve a model which represents this highly nonlinear functionality at best. This model was integrated in the DLR's in-house streamline curvature tool ACDC which is based on the equations of MÖNIG et al. [12], GALLIMORE [8]. The code allows viscous throughflow calculations taking into account radial mixing by turbulent diffusion, endwall boundary layers and a model for tip clearance based on the work of DENTON [7], KRÖGER et al. [9].

Nomenclature

$\dot{m}$	massflow
ϕ	stream line angle from the axial direction $tan\phi = \frac{V_r}{V_x}$
ρ	density
θ	circumferential direction
ε	angle of the quasi orthogonal from the radial direction
E	shear force
k_t	eddy thermal conductivity
p	pressure
ACDC	Advanced Compressor Design Code, preliminary compressor design tool developed in DLR-Institute of Propulsion Technology
AtoB	semi axis relation
b	blockage factor

C Chord length
d thickness
DLR German Aerospace Center
F blade force density
H Duct height
h enthaly
IGV inlet guide vane
M Mach number
m meridional direction
MVDR Meridional Velocity Density Ratio $= \frac{\rho_1 V_{m1}}{\rho_2 V_{m2}}$
q coordinate which is nearly orthogonal to a streamline
r radius
s entropy
T temperature
t Pitch
V Velocity
x axial direction
β_1, β_2 flow angles in relative frame: inflow and outlfow
$\beta_{LE}, \beta_{TE}, \beta_{ST}$ metal angles: leading edge, trailing edge and stagger angle
ω total pressure loss

Subscripts
LE leading edge
t stagnation
TE trailing edge
1 Inflow section, in relative frame
2 Outflow section, in relative frame
c streamline curvature
e empirical
ST Stagger

Introduction

In order to design modern highly loaded and efficient compressors 3D Navier Stokes methods are nowadays indispensable. These methods are very time consuming and need the detailed 3D-geometry. Therefore, 3D design is not suitable for the conceptual phase of the compressor design. Compressor manufacturers have predesign tools which were maintained and developed over many years to be able to analyze and handle their products. The design suite ACDC was developed at DLR-Institute for Propulsion Technology which contains a 0D, 1D and 2D preliminary design tool. A major difficulty in 0D, 1D and 2D performance tools is the prediction of the airfoil performance. In the past most of the pre-design tools predicted the airfoil performance via empirical correlations. These empirical correlations are just accurate for a small range of geometric airfoil design parameters for which they were obtained. Moreover the prediction of airfoil performance at high Mach numbers or at off-design condition is mostly inaccurate. A good overview of existing empirical correlations can be found in ÇETIN et al. [4]. Nowadays, a new approach is needed to consider highly customized, modern airfoil geometries with an increased number of design parameters. MÖNIG et al. [12] recommended to use a database oriented approach for this purpose. In the following work a new method is presented which couples a huge airfoil database with optimized surrogate models for the prediction of the airfoil performance.

Streamline Curvature Throughflow

The throughflow method presented in this work bases mainly on the streamline curvature method of DENTON [6]. The spanwise turbulent mixing model is based on MÖNIG et al. [12] and GALLIMORE [8]. The code is written in C++ and thread parallelized. The method assumes that the flow is:

- adiabatic
- steady
- axisymmetric
- compressible
- Axial Mach number $M_{axial} < 1$

The following models are included to the code

- real gas model
- spanwise turbulent mixing of momentum and heat
- endwall boundary layers
- tip clearance model
- multi flowpath e.g. for splitter configurations

The theory can be outlined as follows:

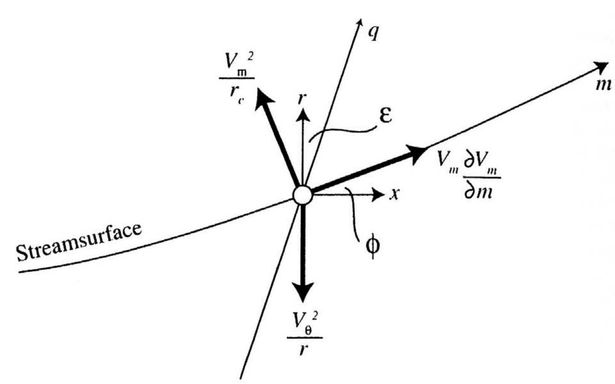

Figure 1. Streamline curvature coordinate system

Consider a fluid particle in the streamline coordinate system, Figure 1. The q-direction describes a coordinate which is nearly orthogonal to a streamline.

The momentum equation in the q-direction is given by (as derived in DENTON [6])

$$\frac{1}{2}\frac{\partial(V_m^2)}{\partial q} = \frac{\partial h_t}{\partial q} - T\frac{\partial s}{\partial q} - \frac{1}{2r^2}\frac{\partial(r^2V_\theta^2)}{\partial q} + V_m\frac{\partial V_m}{\partial m}sin(\varepsilon+\phi) + \frac{V_m^2}{r_c}cos(\varepsilon+\phi) \quad (1)$$

The blade force acting along the quasi orthogonal-q can be neglected. The $V_m\frac{\partial V_m}{\partial m}sin(\varepsilon+\phi)$ and $\frac{V_m^2}{r_c}cos(\varepsilon+\phi)$ terms are solved by evaluating the streamline curvature radius r_c, the angles ε,ϕ and a given initial estimation of V_m. The remaining terms are evaluated by using the energy equation (2) and the streamwise components of the momentum equation in radial and axial direction which can be expressed in terms of a stagnation enthalpy gradient (3). The continuity equation (4) must hold and therefore a given massflow must be reached over all quasi-orthogonals and streamtubes.

$$\frac{\partial s}{\partial m} = \frac{1}{r\rho T V_m}\frac{\partial}{\partial r}\left(rk_t\frac{\partial T}{\partial r}\right) + \frac{\Phi}{\rho T V_m} + \frac{\partial s_e}{\partial m} \quad (2)$$

$$\frac{\partial h_t}{\partial m} = T\frac{\partial s}{\partial m} + \frac{1}{2r^2}\frac{\partial(r^2V_\theta^2)}{\partial m} + \frac{E_x}{\rho}cos(\phi) + \frac{F_m}{\rho} \quad (3)$$

$$\int_{hub}^{tip} 2\pi V_m cos(\varepsilon+\phi)(1-b)dq = \dot{m} \quad (4)$$

To solve the equations (2) and (3) the shear Forces E and the dissipation function Φ must be solved. The derivation of these equations is described in GALLIMORE [8], MÖNIG et al. [12]. The blade forces F_m, F_θ are calculated by knowing the airfoil flow turning and the entropy increase due to the loss coefficients of the airfoil. The complete set of equations can be found in GALLIMORE [8], MÖNIG et al. [12]. As mentioned above the blade rows are represented by total pressure loss coefficient (which is iteratively transformed into an entropy increase)

$$\omega = \frac{p_{t1}-p_{t2}}{p_{t1}-p_1} \quad (5)$$

and the flow turning

$$\Delta\beta = \beta_2 - \beta_1 \quad (6)$$

Most of the streamline curvature tools are using empirical correlations to predict the losses ω and the flow turning $\Delta\beta$. These correlations are in most cases obtained by the use of measured data. Using the correlations is quite simple, fast and stable but they are only accurate for the profiles for which they were obtained and the number of flow and geometrical parameters are quite small (overall about 2-6 parameters) [5, 13, 4, 10].

Another way is the direct coupling of a blade to blade solver with a throughflow solver. The method is called quasi-3D or Q3D WU et al. [15] and it is the most accurate way to calculate the airfoil performance in the conceptual design phase. However this method is numerically unstable and the effort to perform such a calculation in the predesign is quite high.

Novel Approach for Loss and Flow-Turning Prediction

The prediction of loss and flow turning for a given airfoil at a given flow condition is a major difficulty in the preliminary design process. Therefore a functional relationship between the airfoil performance and the geometry/flow condition is needed. A novel approach with the possibility to use more flow and geometrical airfoil parameters than empirical correlations without a loss in stability and speed is the use of surrogate models. Figure 2 shows the use of surrogate models for the prediction of the airfoil performance.

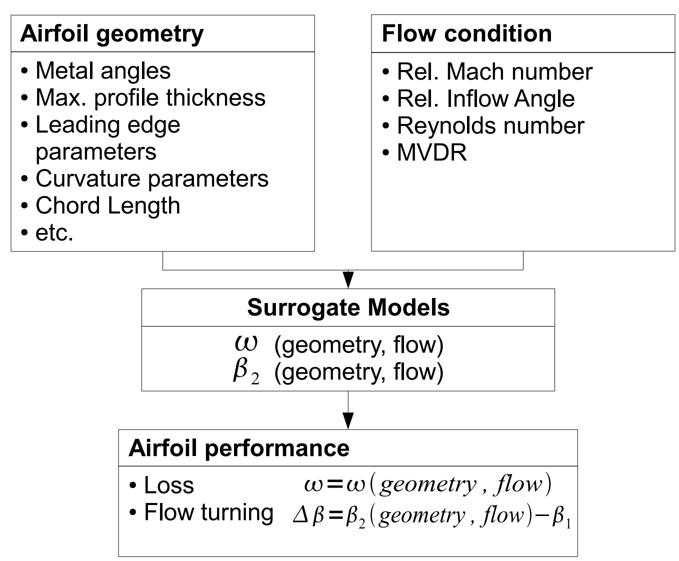

Figure 2. Functional relationship

The input consists on the one hand of the airfoil geometry and on the other hand of the flow condition. The output of the surrogate model is the flow angle and the airfoil losses. Thus the

surrogate model are a response surface for the prediction of the losses $\omega(geometry, flow)$ and the prediction of the flow turning $\beta_2(geometry, flow) - \beta_1$.
One of the major advantages of surrogate models is the ability of generalization. describes the possibility to find relations in available data and draw conclusions for other unknown data.

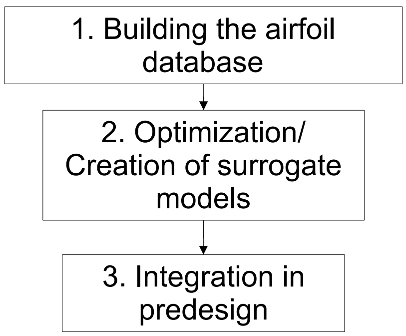

Figure 3. Creation process of a surrogate model

The creation process of the surrogate models is described in Figure 3 and consists of three basic steps.

1. A database with random samples must be created. A random sample is in this case characterized by 10 airfoil geometry parameters, 4 flow parameters and 2 performance parameters. The flow solver that's used for the calculation of the airfoil performance is the blade to blade solver MISES [16]. The framework to create the randomly generated database is the optimization tool AutoOpti, developed at the Institute of Propulsion Technology [14, 2].
2. The second step is the creation and optimization of the surrogate models. The surrogate models are optimized in order to find a surrogate model which describes the airfoil performance at best [2].
3. The third step is the integration of the trained surrogate models in the predesign process. The major application for using the surrogate models is the prediction of airfoil performance by a given geometry and flow conditions. The methodology of 1. and 2. is described in this work. In the future it will also be used to find an optimized airfoil for a given flow turning task.

Building the Airfoil Database

The airfoil database consists of about 10^6 randomly created airfoils also called members or sample points. Each member in the database is described by the 14 input parameters and the 2 output parameters (Table 1).

Input		Output
Flow Parameters	Geometrical parameters	
M_1	β_{LE}	β_2
β_1	β_{TE}	ω
Reynolds nr.	β_{ST}	
MVDR	$\frac{C}{t}$	
	$\frac{d_{max}}{C}$	
	$\frac{d_{maxX}}{C}$	
	x_{DeBoor}, y_{DeBoor}	
	r_{LE}	
	$AtoB$	

Table 1. In- and output parameters of one database member

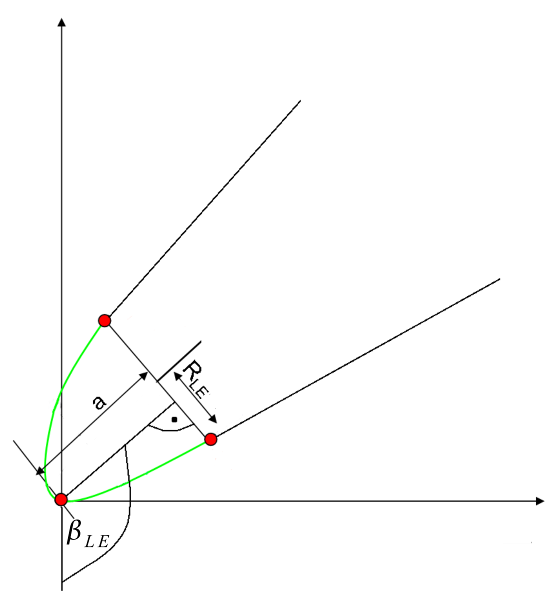

Figure 4. Leading edge parametrization

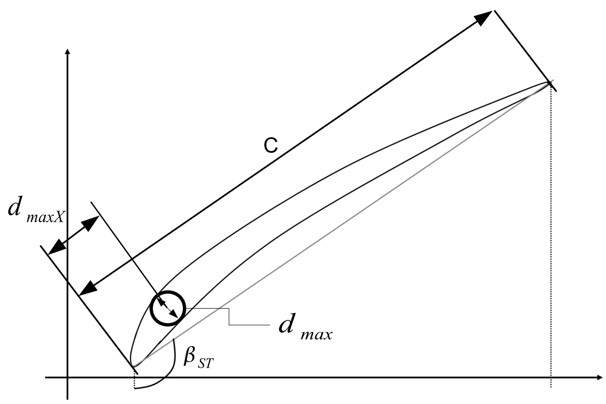

Figure 5. Chord length and stagger angle

The geometrical parametrization for this approach is described by Figure 4 and Figure 5.

- β_{LE} *and* β_{TE} describing the metal angles at the leading edge and trailing edge Figure 4.
- β_{ST} is the airfoil stagger angle Figure 5.
- C is the chord length
- t is the circumferential distance between two airfoils also called pitch
- $\frac{d_{max}}{C}$ is the relative maximum thickness of the airfoil and $\frac{d_{maxX}}{C}$ is the relative axial position of the maximum thickness
- x_{deBoor}, y_{deBoor} describes a spline control point, this point affects the curvature of the airfoil Suction Side
- r_{LE} is the radius of the leading edge of the airfoil
- $AtoB = \frac{a}{r_{LE}}$ is the semi axis ratio, the bluntness of the airfoil can be changed by this value

A more precise description can be found in [14].
Additionally there are several requirements on the database. To find a functional relationship in a 14 dimensional parameter space it is necessary to have a high number of sample points in this space. In this case a large randomly created airfoil database is needed. In order to avoid sparsely sampled regions equally distributed sample points are advantageous for the training of the surrogate models. Hence a random generation of the sample points is a suitable approach. The process to create these sample points is based on 4 steps:

1. Random generation of the flow and the airfoil geometry parameters.
2. Transformation of the geometry parameters to a real airfoil geometry.
3. Calculate a flow solution with the blade to blade flow solver MISES [16].
4. The geometry parameters, the flow parameters and the flow solution are stored in the database for a converged calculation.

The random variation of the airfoil geometry and the flow parameters might result in an uncommon combination of airfoil shape and flow condition. These uncommon combinations are stored into the database in order to have the possibility to predict also bad airfoils. In the future this approach allows an airfoil optimization based on these surrogate models.
The requirements of the database are summarized:

1. A high number of randomly created airfoils (in the presented work: 10^6)
2. Equally spaced sample points
3. Airfoils with a bad performance or unusual geometries are not excluded
4. A large variation of geometrical and flow parameters

Figure 6 shows the distribution of the airfoil losses over the Mach number and the inflow angle for 50.000 randomly selected sample points.

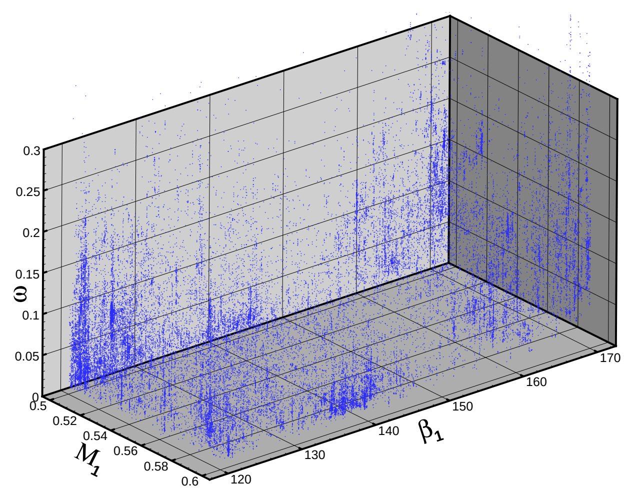

Figure 6. Example of the random parameter distribution

It can be seen that the distribution of the sample points is not entirely uniform. The main reason for this is the creation algorithm of the sample points. The creation algorithm isn't entirely random. In order to speed up the creation process already converged sample points are mutated to create new ones. This algorithm has the benefit of generating more convergent sample points.

Surrogate Models

At DLR-Institute of Propulsion Technology Kriging Models and Neural Networks are used as surrogate models [2]. In this case the usage of a surrogate model which can handle a huge amount of data is advantageous. The training time of Neural Networks linearly depends on the number of sample points $\mathcal{O}(n)$ and Kriging models cubically depends on the number of sample points $\mathcal{O}(n^3)$. Therefore the use of Neural Networks is favorable. The implemented neural networks are Bayesian feed-forward networks [2] and have one output knot.

Bayesian trained Neural Network Bayesian trained neural networks base on the "weight-decay" training algorithm. The "weight-decay" approach is to minimize following function:

$$F = F_D + \lambda F_W = \frac{1}{2}\sum_{i=1}^{D}(f(x_i) - y(x_i,w))^2 + \lambda(\frac{1}{2}\sum_{j=1}^{W} w_j^2) \quad (7)$$

F_D is the sum over D members of the squared error between the neural network output $y(x_i,w)$ and the real fitness values $f(x_i)$ at location x_i (variables of member i). F_W is a measure of the network complexity, represented by the sum of the squared weights. Therefore "weight-decay" tries to find a compromise between fitting the data and reducing the network complexity. The problem is that the solution depends on the regularization constant λ, which has to be estimated.

To use the Bayes'theorem two assumptions are made. Firstly the weights are samples of a normal distribution:

$$p(w) = \frac{\sqrt{\xi}}{\sqrt{2\pi}} e^{-\frac{1}{2}\xi w^2}$$

ξ is the inverse of the variance of the distribution $\xi = \frac{1}{\sigma^2}$.

Secondly the error between network output and real values is also normally distributed:

$$p(f(x) - y(x,w)) = \frac{\sqrt{\nu}}{\sqrt{2\pi}} e^{-\frac{1}{2}\nu(f(x)-y(x,w))^2}$$

ν is the inverse variance of that distribution.

These assumption yields to a new formulation of the "weight-decay" approach (a detailed explanation can be found in [11]):

$$F = \nu F_D + \xi F_w = \frac{\nu}{2}\sum_{n=1}^{N}(y(x^n,w) - t^n)^2 + \frac{\xi}{2}\sum_{q=1}^{W}(w_q)^2$$

$\frac{\xi}{\nu}$ is equivalent to the regularization constant λ and hence the optimal λ can be calculated analytically by using Bayes'theorem (7).

The implemented neural networks are Bayesian feed-forward networks with automatic relevance determination. Thus the weights are divided into subsets with different ξ.

ξ and ν are named hyperparameters.

Splitting of Neural Networks The most simple way to create a Neural Network for the purpose of performance prediction would be the training of one global Neural Network with the whole database. The training time of one Neural Network depends quadratically on the number of weights and in most cases the more sample points are used the more weights are needed. Hence it is advantageous to split the Neural Network in Mach number ranges of 0.1 Mach instead of using one global Neural Network. Table 2 shows that 6 Neural Networks have to be trained in order to predict the outflow angle β_2 and the losses ω for the Mach number range of 0.4-0.7.

Mach number	Neural Networks
0.4 - 0.5	ω *and* β_2
0.5 - 0.6	ω *and* β_2
0.6 - 0.7	ω *and* β_2
0.7 - 0.8	ω *and* β_2

Table 2. Neural Network splitting in Mach number Ranges

Another objective is the prediction of the the outflow angle β_2 and the losses ω at choking condition. Figure 7 shows typical loss and outflow angle functions for a subsonic Mach number $M_1 = 0.65$ and a transonic Mach number $M_1 = 0.95$. At choking condition with a constant inflow Mach number the flow angle β_1 is frozen. It is obvious that this kind of characteristic is no function of the inflow angle $\omega, \beta_2 \neq f(\beta_1, ...)$ anymore and cannot be predicted in this way. The outcome of this is that at transonic flow conditions additional Neural Networks for choking condition have to be trained. Table 3 shows that for one Mach number range at transonic condition 4 Neural Networks have to be trained.

Mach number	Neural Networks	Neural Networks at choke
0.9 - 1.0	ω *and* β_2	ω *and* β_2
1.0 - 1.1	ω *and* β_2	ω *and* β_2

Table 3. Neural Network splitting in transonic Mach number Ranges

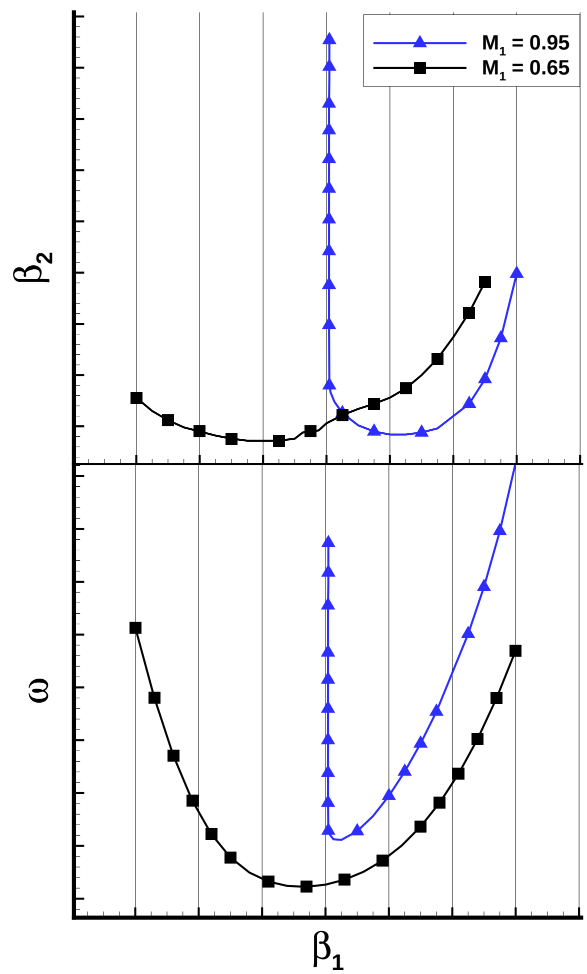

Figure 7. Typical loss and outflow angle Function for a subsonic $M_1 = 0.65$ and transonic $M_1 = 0.95$ airfoil

Optimization of Neural Networks

The prediction quality of a Neural Network is strong associated with its structure (number of knots, layers, weights) and the initial values of the weights and hyper-parameters. The optimization tool AutoOpti [14] was used to improve the prediction quality of the neural networks [2]. AutoOpti is a parallelized optimizer based on asynchronous evolutionary strategies. The free variables for the Neural Network optimization are the number of knots in the hidden layers, the initial values of the hyper-parameters and the connectivity between the input layer and the first hidden layer (from sparsely connected to full connected). Based on experience the connectivity can increase the quality of the prediction. To restrict the time of one Neural Network training, the total number of weights limited to 3000. If the initial Neural Networks consists of more than 3000 weights, they are deleted randomly. The optimization object is to minimize the mean error to a test database (8).

$$MeanError = \sqrt{\frac{1}{N}\sum_{i=1}^{N}(f(x_i) - y(x_i,w))^2} \qquad (8)$$

$(f(x_i) - y(x_i,w))^2$ is the squared error between the test data $f(x_i)$ and the Neural Network prediction $y(x_i,w)$ at the location x_i (variables of member i). N is the number of test data points. This test database is also created randomly and consists of 1000 member. Figure 8 shows the progress of an Neural Network topology optimization. The x-axis shows the optimization progress one number is one bayesian trained Neural Network. On the y-axis the mean error between the Neural Network loss prediction and the test database is shown. The mean error decreases drastically during the optimization obviously.

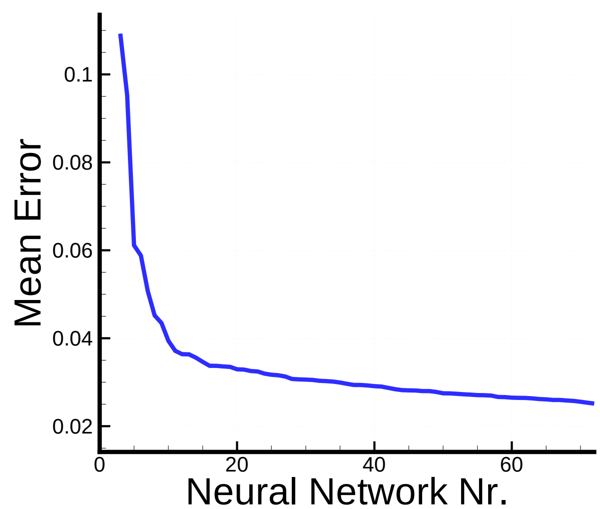

Figure 8. Neural Network loss prediction mean error over the optimization progress

Prediction Results - 4.5 Stage Axial Compressor RIG250

The new approach is verified by comparing the Neural Network predictions with 3D-CFD and 2D-MISES results of rotor 1 of a 4.5 stage transonic compressor providing a total pressure ratio of 4.83 at 46.3 kg/s reduced massflow and 12960 min^{-1} at the design point. The inlet guide vane, stator 1 and stator 2 of this rig are adjustable.

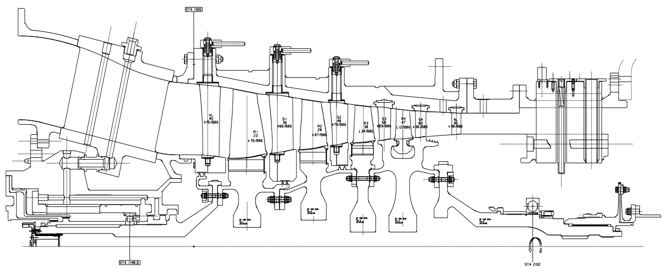

Figure 9. Axial compressor test rig “RIG250” of the DLR - cross section

First of all two speedlines at 80% and 70% RPM were calculated with the 2D Throughflow solver ACDC using the Neural Networks. The results are compared with the 3D-CFD solver TRACE [3, 1]. TRACE is a DLR inhouse 3D-CFD solver which is developed since 20 years and also used and validated by MTU Aeroengines. Secondly the mid section airfoil of rotor 1 (Figure 13) was calculated to compare the results of the Neural Network with the 3D-CFD solver TRACE and the 2D blade to blade solver MISES [16]. Figure 10 shows the analyzation planes used in the CFD calculation. The 2D-Throughflow calculation was made only for Rotor 1 (calculation domain between 1-2), the 3D-CFD calculation also included the IGV. So the inlet condition for the 2D-Throughflow calculation was taken from the 3D solution. 100% RPM was only calculated with the 3D-CFD Code, because the Neural Networks for choking condition are still under development.

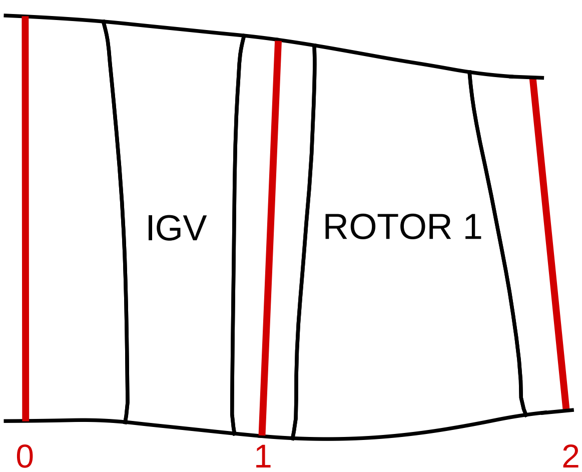

Figure 10. Analyzation planes of the compressor RIG250

Figure 11 shows the performance map of rotor 1 of the compressor RIG250. There is a good agreement between the 3D-CFD and the 2D-Throughflow calculation. Close to small massflows the difference is increasing. This can be explained by the appearance of separation which the simplified boundary layer method of MISES (the Neural Networks are based on MISES Calculations) cannot predict accurately. As mentioned above the Neural Networks currently cannot predict choking condition, so this part of the speedlines is missing.

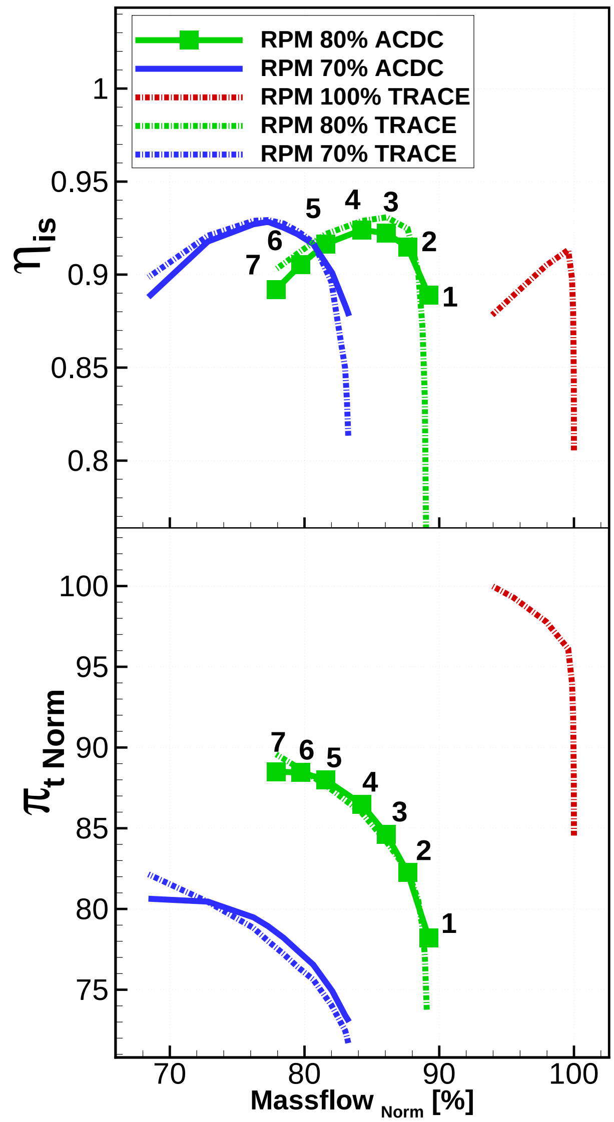

Figure 11. Normalized performance map of Rotor 1, calculated with the 3D-CFD solver TRACE and the 2D-Throughflow solver ACDC

Figure 12 shows the radial distributions of operating points 3 and 6 (cp. Figure 11) at 80% RPM. The inlet Mach number varies between 0.65 at the hub and 1.03 at the tip section, so in the upper 40% relative height of the discussed operation points

3 and 6 has transsonic inflow condition but no choking occurs. The inlet conditions for the 2D-Throughflow solver was taken from the 3D-CFD calculation and given in the absolute frame of reference. The Mach number and the angles in Figure 12 are in relative frame of reference. So the discrepancy in the lower 30%-40% relative height has to come from a slightly different massflow distribution and this may have its origin in the boundary model used in the 2D-Throughflow code. Anyway it is obvious that the predictions of the Neural Networks are describing the Off-Design flow in the correct way. The outflow angle and Mach number is in good agreement with the 3D-CFD solution, also the Off-Design characteristic is in good agreement. The loss distribution shows a correct tendency. In the upper 70% relative height the discrepancy may come from the iterative calculation of the MVDR which is on the one hand an input for the Neural Networks and on the other hand an output of the 2D calculation. The next part of this work shows, that this explanation seems to be probable.

A calculation of the midspan airfoil section of rotor 1 was made. In this case the MVDR is an input which was taken from the 3D CFD calculation, the loss prediction shows better agreement. However the Off-Design characteristic is in good agreement with the 3D-CFD calculations which can also be seen in the outflow Mach number distribution. It should also be emphasized that the airfoils of rotor 1 were not included in the training or test database of the neural networks. The airfoils used for the training of the neural networks are all randomly created, as prescribed in the first part of this work.

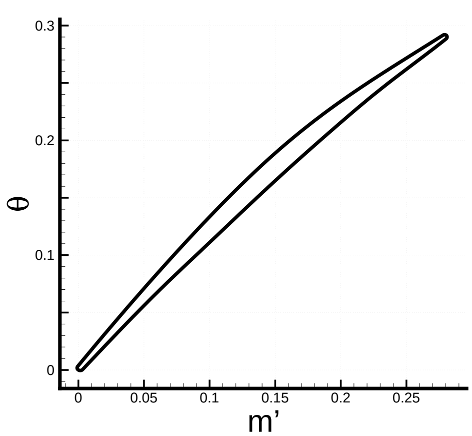

Figure 13. Mid-Section airfoil of Rotor 1 in the m'/θ coordinate system

Table 4 shows the flow parameters of rotor 1 at the different operating points which were compared. These values were obtained from the 3D-CFD calculation and will be used as input for the 2D blade to blade solver and the Neural Networks. The

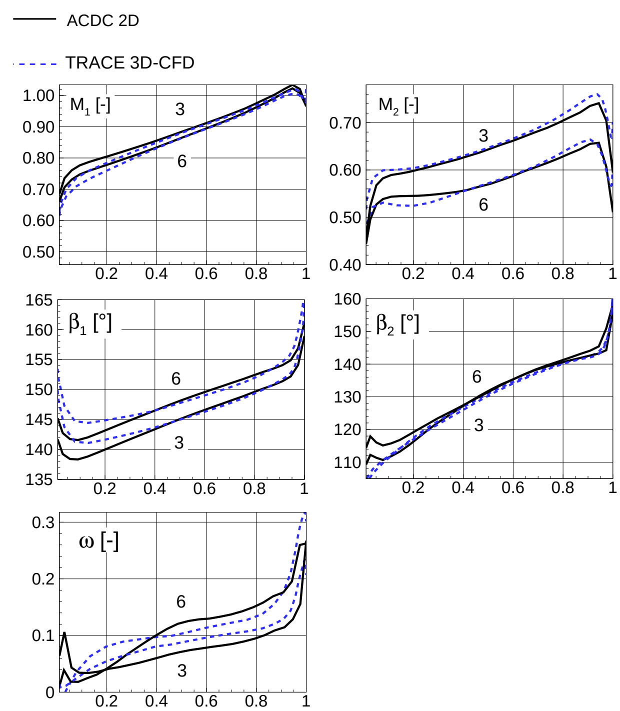

Figure 12. Radial Distribution (r/H) of operating points 3 and 6

numbers in Figure 11 are corresponding with the numbers in Table 4. A MISES definition of the Reynolds number is used, therefore the uncommon high values. The Reynolds number calculated with the common chord length based definition is about $1.6 \cdot 10^6$.

Nr.	β_1	M_1	Reynolds number	MVDR
1	144.76	0.887	$15.5 \cdot 10^7$	1.143
2	144.89	0.886	$15.5 \cdot 10^7$	1.144
3	145.25	0.884	$15.5 \cdot 10^7$	1.143
4	145.94	0.88	$15.5 \cdot 10^7$	1.154
5	146.97	0.874	$15.5 \cdot 10^7$	1.137
6	148.45	0.865	$15.5 \cdot 10^7$	1.123
7	150.65	0.854	$15.5 \cdot 10^7$	1.101

Table 4. Input parameters of comparison points

Table 5 shows the mean error (8) between the test database used in the Neural Network optimization and the Neural Network prediction. Two different Neural Networks for loss prediction (ω) are compared in order to verify the mean error as valid fitness function for the Neural Network optimization. Both Neural Networks are trained with the same database but with different parameters, such as Nr. 67 is more approximative then Nr. 71. Neural Network Nr. 67 is slightly better than Neural Network Nr. 71, hence this Neural Network should produce better results in the comparison.

Neural Network	Mean Error
β_2 Nr. 41	2.539°
ω Nr. 67	0.0251
ω Nr. 71	0.0253

Table 5. Mean Error between a test database of 1000 randomly created airfoils and the Neural Network predictions

Figure 14 shows the comparison between the 3D-CFD solver TRACE, the 2D-blade to blade solver MISES and the Neural Network predictions. The outflow angle β_2 over the inflow angle β_1 is shown on the y-axis in the top frame. On the bottom frame the losses ω over the inflow angle β_1 are shown. In Figure 11 and Table 4 the operating points can be found.

The bottom frame shows a good agreement between the Neural Networks and the 2D-blade to blade solver. The comparison of 2D-blade to blade, Neural Network and the 3D-CFD calculation shows just small differences. Neural Network Nr. 67 shows the better agreement in comparison to Neural Network Nr. 71 and thus the mean error as a quality criteria of the Neural Networks holds. Other calculations showed generally the same agreement. Hence the mean error between a test database and the Neural Network prediction can be recommended as quality criteria.

The top frame shows also a good agreement between the neural networks and the 2D-blade to blade solution. It should be emphasized that the difference of the neural network and the blade to blade solver is in the same dimension as the difference between the blade to blade solver and the 3D-CFD calculations. Thus in this comparison the Neural Network shows a better agreement with the 3D-CFD calculation than with the 2D-blade to blade solver. However the predictions of the Neural Networks bases on sample points which were created with the 2D-blade to blade solver, therefore the Neural Networks should not produce better results than the 2D-blade to blade solver itself. Overall the use in a preliminary design tool like ACDC is suitable.

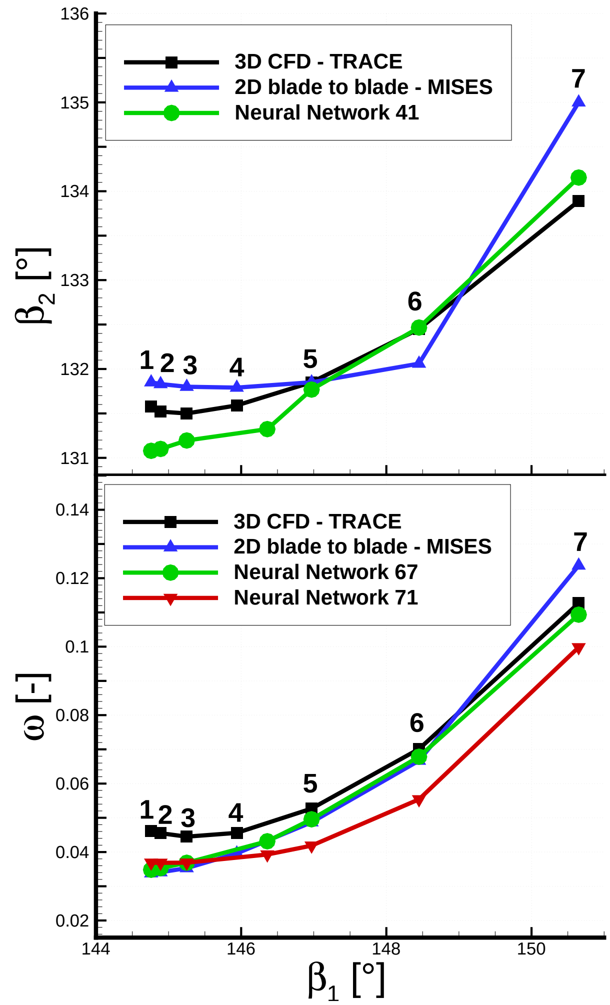

Figure 14. Comparison of 3D-CFD, 2D blade to blade MISES and the Neural Networks of midspan profile Rotor 1 at 80% RPM

Conclusion and Outlook

A novel methodology in predicting the airfoil performance based on a airfoil database and surrogate models is presented.

To create the airfoil database a parametrization has been chosen which can handle already a wide range of airfoil geometries and flow conditions. In the future other parametrizations are possible and will also be tested, in order to extend the range of airfoil geometries and to reduce the amount of data.

An automatic process to build an airfoil database was developed and used to create a database. This process is based on AutoOpti an automatic optimizer developed at DLR-Institute of Propulsion Technology [2, 14]. Based on experience with Metamodels and Optimization, 10^6 sample points have been created and stored inside the database for the training of the surrogate models. The dependency between the prediction accuracy and the number of sample points should be investigated in the future. Furthermore it should be checked if MISES is sufficient as flow solver.

In this work Bayesian trained Neural Networks were chosen as surrogate model because this approach is able to handle a huge amount of sample points. An algorithm to reduce the amount of sample points will be required for the use of other surrogate models such as Kriging. The structure of the Neural Networks was successfully optimized in order to increase the prediction quality of the Neural Networks. The used objective function was tested and validated successfully.

A transonic rotor of the test rig 250 was used to validate the predictions based on the novel methodology. First of all the 2D-Throughflow code ACDC using the neural networks was used to calculate two speedlines of rotor 1 at 80% and 70% RPM. The results are in good agreement with the 3D-CFD calculation. The 100% speedline is missing due to the fact that the surrogate models for choke prediction are still under development. However at 80% RPM rotor 1 is already transsonic. It should be emphasized that the airfoil geometries of rotor 1 were not included to the training or to the test database of the neural networks, all airfoils in the database were randomly created. The prediction of secondary flow effects such as endwall boundary layers and spanwise mixing is still needed.

Secondly a calculation of the rotor 1 midspan airfoil was done in order to compare the blade to blade solver with the surrogate model approach and the 3D CFD calculations more detailed.

Hence the difference of the neural network and the 2D-blade to blade solver is in the same dimension as the difference between the blade to blade solver and the 3D-CFD calculations.

In regard to the input parameters and the accuracy this new methodology is arbitrary expandable. The accuracy can be increased global or just for small areas by adding more sample points to the training. In summary it can be stated that a preliminary design process can be improved in regards to speed and accuracy when using this new methodology.

Further steps in the development of this approach are:

– Include the prediction of performance at choking condition
– Development of the 2D-Througflow solver particularly with regard to the endwall boundary layer method
– Validation for a multistage configuration
– Developing a method for the automatic generation of airfoils out of given performance data based on the created surrogate models
– Development and extension of the airfoil database
– Developing a method of selection for sample points in order to reduce the number of sample points without a loss in accuracy

References

[1] G. ASHCROFT, K. HEITKAMP, and E. KÜGELER. High-order accurate implicit runge-kutta schemes for the simulation of unsteady flow phenomena in turbomachinery. In *V European Conference on Computational Fuild Dynamics ECCOMAS CFD, Lisbon, Portugal*, 2010.

[2] M. AULICH and U. SILLER. High-dimensional constrained multiobjective optimization of a fan stage. In *ASME GT2011-45618*, 2011.

[3] K. BECKER, K. HEITKAMP, and E. KÜGELER. Recent progress in a hybrid-grid cfd solver for turbomachinery flows. In *V European Conference on Computational Fuild Dynamics ECCOMAS CFD, Lisbon, Portugal*, 2010.

[4] M. ÇETIN, AŞ
"UÇER, CH HIRSCH, and GK SEROVY. Application of Modified Loss Correlations to Transonic Axial Compressors. *AGARD Report*, 745, 1987.

[5] HF CREVELING and RH. CARMODY. Axial-flow compressor computer program for calculating off-design performance. *NASA CR*, 72472, 1968.

[6] JD DENTON. Throughflow calculations for transonic axial flow turbines. In *Turbomachinery developments in steam and gas turbines: Presented at the winter annual meeting of the American Society of Mechanical Engineers, Atlanta, Georgia, November 27-December 2, 1977*, page 11. ASME, 1977.

[7] JD DENTON. Loss mechanisms in turbomachines. *Journal of Turbomachinery*, 115(4):621–656, 1993.

[8] SJ GALLIMORE. Spanwise Mixing in Multistage Axial Flow Compressors: Part II—Throughflow Calculations Including Mixing. *Journal of Turbomachinery*, 108:10, 1986.

[9] G. KRÖGER, C. CORNELIUS, and E. NICKE. *Beeinflussung der Spaltströmung durch Optimierung der Geometrie im Schaufelspitzenbereich*. AG-Turbo Abschlussbericht, COORETEC-TURBO Teilvorhaben 1.2.1 des Verbundprojektes CO2-Reduktions-Technologien, September 2009. Förderkennzeichen 0327715 A.

[10] S. LIEBLEIN and NACA. GLENN RESEARCH CENTER. *Analysis of Experimental Low-Speed Loss and Stall Characteristics of Two-Dimensional Compressor Blade Cascades*. National Advisory Committee for Aeronautics, 1957.

[11] D.J.C. MACKKAY. *Bayesian methods for adaptive models*. PhD thesis, Citeseer, 1991.

[12] R. MÖNIG, F. MILDNER, and R. RÖPER. Viscous-Flow Two-Dimensional Analysis Including Secondary Flow Effects. *Journal of Turbomachinery*, 123:558, 2001.

[13] CC OCH and LH. SMITH JR. Loss sources and magnitudes in axial-flow compressors. *ASME Journal of Engineering for Power*, 98(3):411–424, 1976.
[14] C. VOß. *Automatische Optimierung von Verdichterschaufeln*. Abschlussbericht zum AG-Turbo COOREFF-T Teilvorhaben 1.1.1 des Verbundprojektes CO2-Reduktion durch Effizienz, 2008. Förderkennzeichen 0327713 B.
[15] C.H. WU, NATIONAL AERONAUTICS, and SPACE ADMINISTRATION WASHINGTON DC. A General Theory of Three-Dimensional Flow in Subsonic and Supersonic Turbomachines of Axial-, Radial, and Mixed-Flow TYpes. 1952.
[16] H. YOUNGREN and M. DRELA. Viscous/inviscid method for preliminary design of transonic cascades. In *AIAA, SAE, ASME, and ASEE, Joint Propulsion Conference, 27 th, Sacramento, CA*, page 1991, 1991.